Experimental demonstration of negative refraction imaging in both amplitude and phase

Zhaolin Lu, Shouyuan Shi, Christopher A. Schuetz, and Dennis W. Prather

Department of Electrical and Computer Engineering,
University of Delaware, Newark, DE 19716,USA
dprather@ee.udel.edu

http://www.ece.udel.edu/~dprather/

Abstract: We studied a two-dimensional square-lattice photonic crystal with all-angle negative refraction at its first band. Using this photonic crystal, we designed and fabricated a flat lens functioning as a cylindrical lens by increasing the vertical dimension of the photonic crystal. Two-dimensional finite-difference time-domain simulation validated negative refraction imaging. To perform the experiment, a microwave imaging system was built based on a vector network analyzer. Field distributions were acquired by scanning the imaging plane and object plane. The experiment demonstrated negative refraction imaging in both amplitude and phase, and obtained an image with feature size, $0.77\lambda_0$.

OCIS codes: (999.9999) Negative refraction, (999.9999) Photonic Crystal, (999.9999) Flat lens, (110.2990) Image formation theory, (100.6640) Super resolution, (220.3620) Lens design, (120.5050) Phase measurement

References and links

1. V.G. Veselago, "The electrodynamics of substances with simultaneously negative values of permittivity and permeability." Sov. Phys. Usp. **10**,509-514(1968).
2. J.B. Pendry, A.J. Holden, W.J. Stewart and I. Youngs, "Extremely low frequency plasmons in metallic mesostructures." Phys. Rev. Lett. **76,** 4773–4776 (1996).
3. J.B. Pendry, A.J. Holden, D.J. Robbins, and W.J. Stewart, "Magnetism from conductors and enhanced nonlinear phenomena." IEEE Trans. Microw. Theory Techniques. **47,** 2075–2084 (1999).
4. R.A. Shelby, D.R. Smith, and S. Schultz, "Experimental verification of a negative index of refraction." Science, **292**, 77-79 (2001).
5. M. Notomi, "Theory of light propagation in strongly modulated photonic crystals: refractionlike behavior in the vicinity of the photonic band gap." Phys. Rev. B. **62,** 10696-10705 (2000).
6. P.V. Parimi, W.T. Lu, P. Vodo, J. Sokoloff, J.S. Derov, and S. Sridhar, "Negative refraction and left-handed electromagnetism in microwave photonic crystals." Phys. Rev. Lett. **92**, 127401(4) (2004).
7. E. Cubukcu, K. Aydin, E. Ozbay, S. Foteinopoulou, and C.M. Soukoulis, "Electromagnetic wave: negative refraction by photonic crystals." Nature, **423**, 604-605 (2003).
8. J.B., Pendry, "Negative refraction makes a perfect lens." Phys. Rev. Lett. **85**, 3966-3969 (2000).
9. N. Garcia1, and M. Nieto-Vesperinas, " Left-handed materials do not make a perfect lens." Phys. Rev. Lett. **88**, 207403(4) (2002).
10. P.M. Valanju, R. M. Walser, and A. P. Valanju, " Wave refraction in negative-index media: always positive and very inhomogeneous." Phys. Rev. Lett. **88**, 187401(4) (2002).
11. N. Garcia, and M. Nieto-Vesperinas, "Is there an experimental verification of a negative index of refraction yet?" Opt. Lett., **27**,885-887(2002).
12. J. B. Pendry, "Positively negative." Nature, **423**, 22(2003).
13. C. Luo, S.G. Johnson, J.D. Joannopoulos, and J.B. Pendry, "All-angle negative refraction without negative effective index." Phys. Rev. B, **65,** 201104(R) (2002).
14. P.V. Parimi, W.T. Lu, P. Vodo, and S. Sridhar, "Photonic crystals: imaging by flat lens using negative refraction." Nature, **426**, 404 (2003).
15. H. Kosaka, T. Kawashima, A. Tomita, M. Notomi, T. Tamamura, T. Sato, and S. Kawakamib, "Self-collimating phenomena in photonic crystals", Appl. Phys. Lett. **74**, 1212-1214 (1999).

#6574 - $15.00 US Received 8 February 2005; revised 7 March 2005; accepted 7 March 2005

16. C. Luo, S.G. Johson, J.D. Joannopoulos, and J.B. Pendry, "All-angle negative refraction in a three-dimensionally periodic photonic crystal." Appl. Phys. Lett. **81**, 2352-2354 (2002).
17. X. Ao and S. He, "Three-dimensional photonic crystal of negative refraction achieved by interference lithography." Opt. Lett., **29**, 2542-2544(2004).

1. Introduction

In 1968, V.G. Veselago argued that if both permittivity and permeability were negative, it follows that the refractive index of the material would also be negative [1]. In this material, the electric field **E**, magnetic field **H**, and the propagation constant **k** are not composed of a set of right-handed coordinates, but left-handed coordinates. Therefore, he called this material left-handed material (LHM). The most remarkable thing for a LHM is that the group velocity is opposite to the phase velocity when electromagnetic waves propagate in it. Also, since the refractive index is negative, the refracted beam will bend to the "wrong" way when a beam is incident into this material from a common material (right-handed material). This phenomenon is "negative refraction". Using negative refraction, one could make a lens with flat surface. Veselago also suggested that it was possible to find this material in plasmas. Pendry *et al* [2] studied interlaced wire structure and concluded that their structure resembles plasma, but has very low effective electron density and very high effective electron mass, resulting in a plasma frequency as low as GHz's. In particular, it is possible to achieve negative permittivity at microwave regime by tuning its period. Based on the same philosophy, they proposed another structure made of periodic metal rings and showed negative permeability can also be achieved [3]. Shelby *et al* experimentally demonstrated negative refraction by a structure combining the interlaced wires and the periodic rings [4]. Meanwhile, Notomi [5] studied the dispersion behavior in the vicinity of the photonic band gap and simulated that negative refraction can also be achieved in a dielectric photonic crystal(PhC). Parimi *et al* [6] and Cubukcu *et al* [7] experimentally demonstrated the negative refraction in dielectric photonic crystals.

Pendry's another work sparked significant interest in negative refraction and the flat lens—"Negative refraction makes a perfect lens" [8]. He explained that negative refraction amplifies evanescent waves, and both propagating and evanescent waves contribute to the resolution of the image. Garcia1 *et al* argued that negative refraction does not make a perfect lens because the finite thickness of a lens prevents the restoration of evanescent waves and perfect focusing [9]. In fact, there are more debates ever since the concept of negative refraction was proposed. Several years ago, negative refraction as a basic physical phenomenon was discussed intensely in physics and optics. The debates among scientists were then focused on whether negative refraction is possible and how it would work [10-12]. Nowadays, more interest in imaging by negative refraction has arisen in material science, RF engineering, electrical engineering, optical communication, and medical engineering. A key problem is whether a "perfect lens" can be achieved by negative refraction. Our work is aimed at answering this question.

2. " Flat cylindrical" lens

In our work, we use a two-dimensional (2D) photonic crystal to demonstrate negative refraction imaging. The key distinctions of this work lie in designing the photonic crystal at the first band [13], increasing the vertical dimension of the flat lens, and validating the imaging in both amplitude and phase. Although imaging by a flat lens using negative refraction has been demonstrated in 2D photonic crystals formed by arranging alumina rods in the air [14], the phase distribution has not been reported yet, which is a very important and convenient criterion to validate the imaging when a point object is used. In addition, the assembled "rods-in-air" flat lens is not convenient for fabrication and applications. Its small dimension on vertical direction also limits its practical applications.

Instead of fabricating holes in a thin dielectric slab or assembling short rods between two metal plates to form a photonic crystal allowing only single mode on the vertical direction, we increased the vertical dimension of the photonic crystal until this dimension can be treated as

#6574 - $15.00 US Received 8 February 2005; revised 7 March 2005; accepted 7 March 2005

infinite to avoid the reflection on vertical direction, as shown in Fig. 1(a). As a result, we proposed a lens with flat surfaces and functioning as a cylindrical lens, namely "flat cylindrical" lens. For designing a planar photonic crystal, a widely used method is to apply an effective index into 2D calculations and simulations. However, the effective index is always smaller than the bulk material refractive index. Thus, a poor index contrast results, which is often a problem for designing photonic crystal flat lens. In contrast, our approach has the advantage in that larger index contrast is available because we applied the bulk refractive index, instead of the effective index, to calculate the equi-frequency contours (EFC) and simulate the behavior of the electromagnetic wave in the horizontal plane (the zero-spatial frequency component) using the 2D finite-difference time-domain (FDTD) method. Theoretically, this approach is a better approximation to the 2D configuration as the device has no limitation on the vertical direction, and the wave propagating on the vertical direction is excluded.

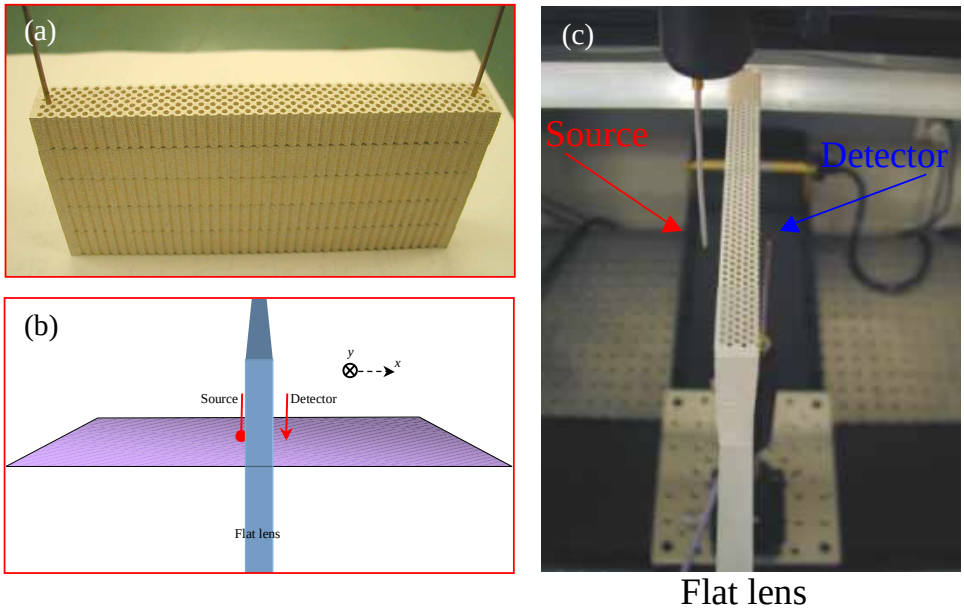

Fig. 1. (a) Picture of the fabricated flat lens. (b) Illustration of the experimental setup. The source is located at x= -1. (c) Picture of the experimental setup.

3. Negative refraction at the first photonic band

A square-lattice of air holes in dielectric ε=15, with lattice constant a, and hole diameter $2r$=0.70a is employed in our work. C. Luo, *et al* have theoretically investigated the dispersion properties of a similar photonic crystal and numerically simulated negative refraction imaging by the photonic crystal [13]. Our work is focused on experimental demonstration. However, we summarize some key points of the theoretical analysis for understanding the imaging mechanism and experimental results. We used the plane wave expansion method to solve the corresponding eigen frequencies for a given wave vector. Figures 2(a), 2(b) and 2(c) show the photonic band diagram, photonic band structure and equi-frequency contours, respectively. By observing the EFCs, we can see that all-angle negative refraction in the first band occurs at normalized frequencies of ω_n=0.17~0.20 because at these frequencies the EFCs are all-convex. By its definition, the excited mode will propagate with group velocity $\mathbf{v}_g = \nabla_{\mathbf{k}}\omega(\mathbf{k})$ [15], which means the group velocity is always perpendicular to the EFC. As a result, the group velocity is not opposite to its phase velocity in our case. However, negative refraction

#6574 - $15.00 US Received 8 February 2005; revised 7 March 2005; accepted 7 March 2005

still occurs at its first band. C. Luo *et al* attributed this to its *negative-definite photon effective mass*[13].

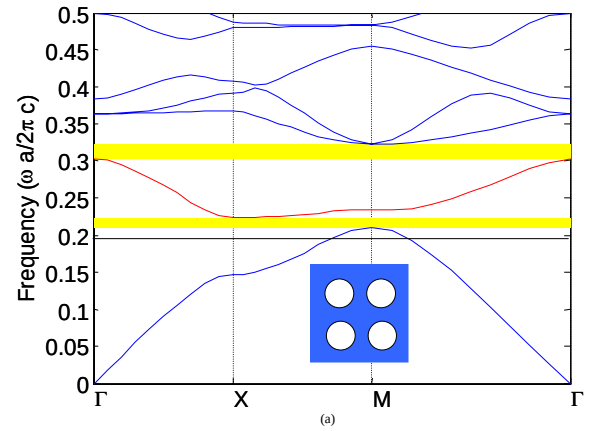

(a)

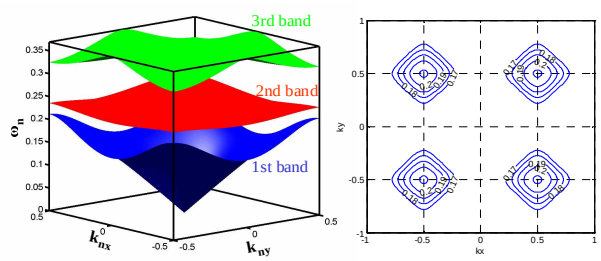

(b) (c)

Fig. 2. (a) TE mode dispersion diagram of the square-lattice PhC. (b)TE mode photonic band structure of the square-lattice PhC. (c)TE mode EFCs of the square-lattice PhC at the vicinity of the first bandgap.

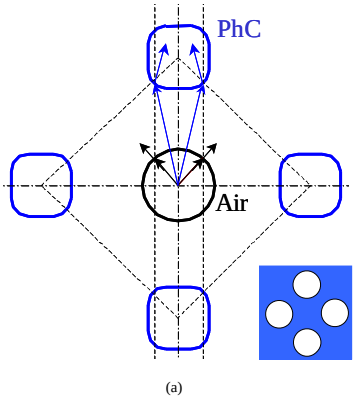

(a)

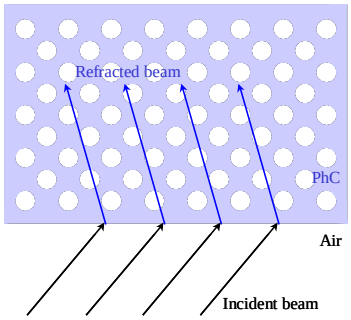

(b)

Fig. 3.(a) Illustration of propagation of the incident beam and refracted beam in k-space. (b) Illustration of propagation of the incident beam and refracted beam in real space.

Figure 3(a) shows how this occurs in **k**-space: when a light beam is incident from the air into the photonic crystal, the tangential component of the wave vector (phase velocity) is continuous at the interface and the group velocity is perpendicular to the EFC. As a result, k_x component bends to reverse direction and k_y component keeps its direction. The group velocity is only "partially" opposite to its phase velocity. However, the light beam still bends to a "wrong" direction, which is negative refraction. Figure 3(b) shows how negative refraction occurs in the real space. In addition, the EFCs at ω_n=0.17~0.20 are all-convex, which means the photonic crystal can gather incident beams from all direction and form an image.

Based on these observations, we simulated a flat lens made of this photonic crystal: the hole diameter is 2*r*=1.6mm, the lattice constant is *a*=1.6/0.7=2.3mm, the thickness of the lens is 14.5mm, and the working frequency is *f*=24.6GHz(λ_0=12.2mm), which corresponds to normalized frequency ω_n=0.19. The flat lens works at the first band and the optical axis is designed along (1,1). Figures 4a and 4b show the simulated phase and amplitude distributions. From Fig. 4, we can see that an image is really formed by the negative refraction using this flat lens. The lateral size of the simulated image is 9mm or 0.7λ.

4. Experiment

In our work, a computer numerically controlled (CNC) micro-milling machine is used to fabricate the flat lens. Figure 1a shows the photonic crystal lens we fabricated. The square-lattice photonic crystal, as a flat lens, is fabricated in a low loss material with dielectric

#6574 - $15.00 US Received 8 February 2005; revised 7 March 2005; accepted 7 March 2005

constant 15. It has the same parameters as the flat lens we simulated, i.e., $2r$=1.6mm, a=1.6/0.7=2.3mm, the thickness of the lens=14.5mm. In addition, its dimension at vertical direction is 63.5mm, which is much larger than the lens thickness.

We have built a microwave imaging setup, as illustrated and shown in Fig. 1(b) and 1(c), based on an Agilent 85106D vector network analyzer, which encompasses a test and measurement capability spanning 45MHz through 110GHz. A particularly attractive feature of this system is its ability to measure results in both amplitude and phase. The source is a dipole antenna connected to the network analyzer, and the detector is another dipole antenna fed back to the network analyzer. The detector is mounted on an *X*-*Y* scanner to map the electric field. The field distribution is acquired by scanning the object plane and image plane. A custom program was developed to synchronize the scanning and measurement. Once a scanning and measurement is finished, we depict the S-parameter value, S_{21} in our case, with regard to the position as an image. Consequently, each pixel in the image corresponds to the S-parameter value at a scanning position. In addition, in the network analyzer the S-parameter is given as complex values, so we can obtain both amplitude and phase distributions, which is impractical for near infrared or visible light measurement.

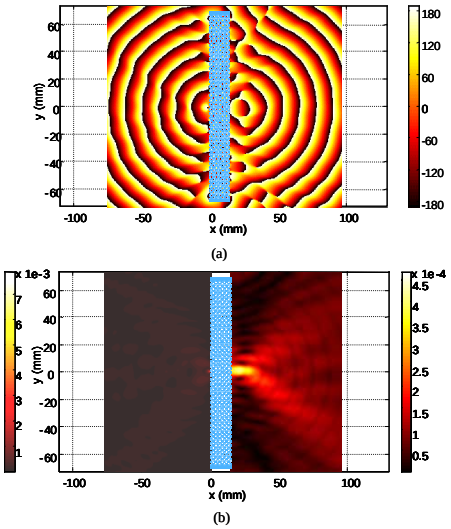

Fig. 4. (a) Simulated phase distribution (unit: radian) when a dipole is placed at object distance 1mm: TE mode at 24.6GHz. (b) Simulated amplitude distribution when a dipole is placed at object distance 1mm: TE mode at 24.6GHz.

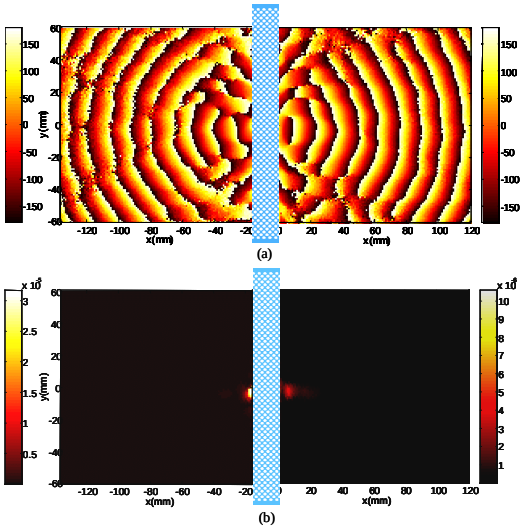

Fig. 5. (a) The measured phase distributions (in degrees) at 23.2GHz for the source (left) and the image (right). The flat lens (photonic crystal) is depicted between the source and the image. (b) The measured amplitude distributions at 23.2GHz. The flat lens (photonic crystal) is depicted between the source and the image.

To perform the experiment, we placed the source dipole 1mm away from the lens, with the electric component polarizing along *y*-axis to stimulate a transverse-electric mode, and mapped the field distribution using the *X*-*Y* robot, meanwhile spanning the frequencies from 22GHz to 26GHz with spacing 0.2GHz. Consequently, we observed good images in the frequency range of 23.2±0.6GHz. Figures 5(a) and 5(b) show the measured phase and amplitude distributions for 23.2GHz. From the measured amplitude distribution, we can see that a high amplitude spot appears on the image plane. From the measured phase distribution, we can see that a closed circle appears on the image plane, which precludes the possibility that the small spot is observed because the detector is close to the source. According to this point, our result more strongly supports negative refraction imaging than the result reported [14]. Therefore, from the amplitude distribution and particularly from the phase distribution, we validate that waves *converge* to form an image at 7mm away from the lens at the imaging side, and then *diverge* into far field. The lateral size of the image is about 10mm, which is 77% of the corresponding wavelength, 13mm. In contrast, it is well known that a conventional

#6574 - $15.00 US Received 8 February 2005; revised 7 March 2005; accepted 7 March 2005

lens cannot focus microwave or light on an area smaller than a square wavelength [8]. The reduction of the intensity between the image and object may be attributed to the divergence on vertical direction and back reflection.

In addition, there is little change with the image when we shifted the detector ±2mm along the vertical direction. Although this is far from obtaining 3D imaging, the large vertical dimension of the flat lens opens the door for another dimension, as well as practical applications. Without another dimension, the flat lens can have few practical applications. Once another dimension is introduced, the photonic crystal flat lens can be directly used in microwave imaging, and optical imaging systems. This issue can be resolved by fabricating 3D photonic crystals [16,17].

5. Conclusions

To summarize, we designed, simulated, fabricated and characterized a flat lens, which works by negative refraction and functions as a cylindrical lens. For the first time, the experiment demonstrated the negative refraction image of a point source in both amplitude and phase. By analyzing the image field distribution, we measured the image feature size to be $0.77\lambda_0$. However, as we claimed in section 4 the group velocity is not opposite to its phase velocity in our case. Effective index $n_{\text{eff}} = -1$ cannot be achieved in our structure. As a result, index matching and aberration are exacerbated in negative refraction imaging. Our recent experiment on a triangular-lattice PhC demonstrated negative refraction imaging with $n_{\text{eff}} = -1$. We will report it in the future.

#6574 - $15.00 US Received 8 February 2005; revised 7 March 2005; accepted 7 March 2005